Research Article

Novel Mannan-PEG-PE Modified Bioadhesive PLGA Nanoparticles for Targeted Gene Delivery

Guicun Wu,[1] Fang Zhou,[2] Linfu Ge,[2] Ximin Liu,[2] and Fansheng Kong[2]

[1] *Department of Hematology, Shandong Provincial Crops Hospital, Chinese People's Armed Forces, Jinan, China*
[2] *Department of Hematology, General Hospital of Jinan Command, PLA, Jinan, 250031, China*

Correspondence should be addressed to Fansheng Kong, kongfanshengphd@yahoo.com.cn

Purpose. Biodegradable polymeric nanoparticles have been used frequently as gene delivery vehicles. The aim of this study is to modify bioadhesive PLGA nanoparticles with novel synthetic mannan-PEG-PE (MN-PEG-PE) to obtain active targeted gene delivery system. *Methods.* Mannan-PEG-PE ligands were synthesized and modified onto the NPs/pEGFP complexes. The modification rate was optimized, and the characteristics of the vehicle were evaluated. Then, the modified vectors were intravenous delivered to rats, and *in vivo* targeting behavior of MN-PEG-PE modified PLGA nanoparticles/pEGFP complexes (MN-PEG-PE-NPs/pEGFP) in liver macrophages was investigated. *Results.* MN-PEG-PE-NPs/pEGFP displayed remarkably higher transfection efficiencies than nonmodified NPs/pEGFP both *in vitro* and *in vivo*. *Conclusions.* Mannan containing targeting ligands could significantly improve the transfection efficiency of the carriers. MN-PEG-PE modified vectors very useful in targeted gene delivery.

1. Introduction

Nonviral pharmaceutical vectors, such as polymeric nanoparticles, liposomes, micelles, nanocapsules, solid lipid nanoparticles, niosomes, and other vectors, have been widely used for drug/gene delivery because they are less toxic, less immunogenic, and easy to be modified [1–5]. Biodegradable polymeric nanoparticles have been used frequently as gene delivery vehicles due to their extensive bioavailability, better encapsulation, high stability, and minimal toxicity [6, 7]. They can be tailor-made to achieve both controlled drug release and active targeting by tuning the polymer characteristics and shaping the surface through nanoengineering [8, 9]. A number of different polymers, both synthetic and natural, have been utilized in formulating biodegradable nanoparticles [10–14].

One of the most extensively investigated polymers for nanoparticles is the biodegradable and biocompatible poly (D,L-lactide-co-glycolide) (PLGA), which has been approved by the FDA for certain human clinical uses [15]. In our previous study, a novel mannan modified DNA loaded bioadhesive PLGA nanoparticles (MAN-DNA-NPs) were investigated for targeted gene delivery to the rats Kupffer cells (KCs)

[16]. Bioadhesive PLGA nanoparticles were prepared and subsequently bound with pEGFP. Following the coupling of the mannan-based PE-grafted ligands (MAN-PE) with the DNA-NPs, the MAN-DNA-NPs were delivered intravenously to rats and achieved high *in vivo* transfection efficiency. So PLGA nanoparticles modified with mannan could be a promising carrier for gene delivery.

Poly(ethylene glycol) (PEG) modification of nanocarriers have emerged as common strategies to ensure stealth shielding and long-circulation and could also provide the nanocarriers active targeting properties by covalent attached with the wide assortment of targeting ligands by amide bonding or disulfide bridge formation [17]. A series of PEG containing ligands commonly named PEG-phosphatidylethanolamine (PEG-PE) conjugates were reported by Torchilin's group. They demonstrated that PEG-PE conjugates with various PEG lengths and terminal targeted moieties can provide extremely stable, long-circulating, and active-targeting nanocarriers spontaneously accumulate in specific sites [4, 18, 19]. Then PEG-PE was widely used in nanoparticulate formulations [20, 21]. After that, several ligands i.e. PEG-PE (TAT-PEG-PE for instant) were also applied for targeted delivery of drugs/genes [22–24].

In this study, a novel conjugated ligand mannan-PEG-PE (MN-PEG-PE) was synthesized, and MN-PEG-PE modified bioadhesive PLGA nanoparticles were investigated as active targeted gene delivery system using plasmid enhanced green fluorescent protein (pEGFP) as the model gene. The novel modified vectors were intravenous delivered to rats and *in vivo* targeting behavior of MN-PEG-PE modified PLGA nanoparticles/pEGFP complexes (MN-PEG-PE-NPs/pEGFP) in liver macrophages was investigated in comparison with non-modified NPs/pEGFP complexes and Lipofectamine 2000/pEGFP (Lipo/pEGFP) complexes.

2. Materials and Methods

2.1. Materials. Poly(D,L-lactic-*co*-glycolic) (PLGA, 50 : 50, Av. MW 25,000) was obtained from Shandong Institute of Medical Instrument (China). Butyl carbonyl (Boc)-NH-PEG$_{2000}$-COOH was purchased from Shanghai Yarebio Co., Ltd. (China). Mannan, L-α-phosphatidylethanolamine (PE), Concanavalin A (Con A), and MTT (3-[4,5-dimehyl-2-thiazolyl]-2,5-diphenyl-2H-tetrazolium bromide) were purchased from Sigma-Aldrich Co., Ltd. (USA). pEGFP-N1 was provided by Shandong University (China). Quant-iT PicoGreen dsDNA quantitation reagent and Lipofectamine 2000 were obtained from Invitrogen by Life Technologies (USA). All other chemicals were of analytical grade or higher.

2.2. Animals. Adult male Sprague Dawley rats (10 to 12 weeks old) were purchased from the Medical Animal Test Center of Shandong Province and housed under standard laboratory conditions. All animal experiments complied with the requirements of the National Act on the Use of Experimental Animals (People's Republic of China).

2.3. Synthesis of MN-PEG-PE Ligands. MN-PEG-PE ligands were synthesized as described in Figure 1. Boc-NH-PEG-COOH (100 mg) was dissolved with dimethyl sulfoxide (DMSO) and stirred with PE (36 mg) as a mixture. 1-[3-(dimethylamino)propyl]-3-ethylcarbodiimide (EDC·HCl) (72 mg) and triethylamine (TEA, 1 equivalent of EDC·HCl) were dissolved in DMSO and added dropwise into the mixture in an ice bath, stirred for 36 hours, then the concentrated hydrochloric acid was used to detach the Boc group, to produce NH$_2$-PEG-CO-NH-PE. Mannan (100 mg) was dissolved with sodium hydroxide (1 M, 1 mL) and stirred for 30 min for alkalinization, then chloroacetic acid (20%, 1 mL) was added into the solution and stirred in an oil bath (60°C) for 6 h. After that, hydrochloric acid (1 M) was added until pH 2-3 to complete the carboxymethylation of mannan [25]. Carboxymethylated mannan was then stirred with NH$_2$-PEG-CO-NH-PE in DMSO solution, and EDC·HCl mixed with TEA (1 equivalent of EDC·HCl, in DMSO) were added dropwise into the solution in an ice bath, stirred for 24 hours. DMSO was moved by rotary evaporation, and the product was dialyzed against *Milli-Q* water for 24 hours to finally form MN-PEG-PE. The structure of MN-PEG-PE was confirmed by IR and ^{1}H NMR spectroscopy. IR ν/cm^{-1}: 3517.3 (-NH-, -OH); 1820.4 (-C=O); 1667.9 (-HN-CO-);

1635.2 (-HN-CO-). ^{1}H NMR (DMSO-d6, 300 MHz) δ: 2.47 (CH$_2$CO), 3.26 (CH$_2$N) 6.05 (NH).

2.4. Preparation of pEGFP Loaded Bioadhesive PLGA Nanoparticles. Bioadhesive PLGA nanoparticles (NPs) were prepared following the methods described previously by our group [16]. Briefly, Carbopol 940 (CP) was dispersed in distilled water at room temperature and left overnight to swell. Required amount of 1 M NaOH was added to neutralize the dispersion until pH 7.0 was reached and diluted with distilled water to afford a 0.02% (w/v) CP solution. Bioadhesive PLGA nanoparticles were prepared under optimized conditions by a nanoprecipitation method (solvent displacement technique) [26, 27]. 50 mg of PLGA polymer was accurately weighted and dissolved in 3 mL acetone. The organic phase was added dropwise into the 0.02% CP solution being stirred at 600 rpm at room temperature. When complete evaporation of the organic solvent had occurred, the redundant stabilizers and the nanoparticles were separated by ultracentrifugation at 1000 g, 4°C for 20 min. The pellet was resuspended in Milli-Q water, washed three times, and filtered through a 0.45 μm membrane.

The reporter gene pEGFP was mixed with the PLGA nanoparticles by vortexing the nanoparticle suspension with a 1 mg/mL solution of DNA for 20 s. Incubation of the mixture for 30 min at RT facilitated the formation of the pEGFP-loaded PLGA nanoparticles (NPs/pEGFP) (Figure 2).

2.5. Modification of NPs/pEGFP with MN-PEG-PE. MN-PEG-PE modified NPs/pEGFP complexes (MN-PEG-PE-NPs/pEGFP) were produced by solvent diffusion method (Figure 2) [28, 29]. Briefly, MN-PEG-PE ligands were dissolved in 2 mL of phosphate buffered saline (PBS, pH 7.4). Then the solution was added dropwise into 10 mL of NPs/pEGFP complexes that was stirred at 600 rpm at RT leading to the immediate modification. Subsequently, free MN-PEG-PE was removed from modified NPs/pEGFP by gel chromatography using a Sephadex G-50 column (GE Healthcare, Sweden). The obtained complexes were resuspended in Milli-Q water, washed three times, and filtered through a membrane with 0.80 μm pore size to obtain MN-PEG-PE-NPs/pEGFP. To optimize the modification ratio, MN-PEG-PE ligands dissolved in PBS were designed at different weight rate to the NPs/pEGFP (w/w). The particle sizes and zeta potential of complexes were determined using a Zetasizer Nano-ZS instrument (Malvern Instruments, UK).

2.6. Determination of MN-PEG-PE Modification. To confirm the success of modification and determine the best ratio of MN-PEG-PE to NPs/pEGFP, several experiments were carried out.

2.6.1. Particle Sizes Determination and PicoGreen-Fluorometry Assay. During the modification procedure, MN-PEG-PE ligands were coated onto the NPs/pEGFP carriers due to the bioadhesive property of CP coated on the surface of the NPs. Theoretically, the more ligands modified onto the carriers, the better targeted delivery ability they will
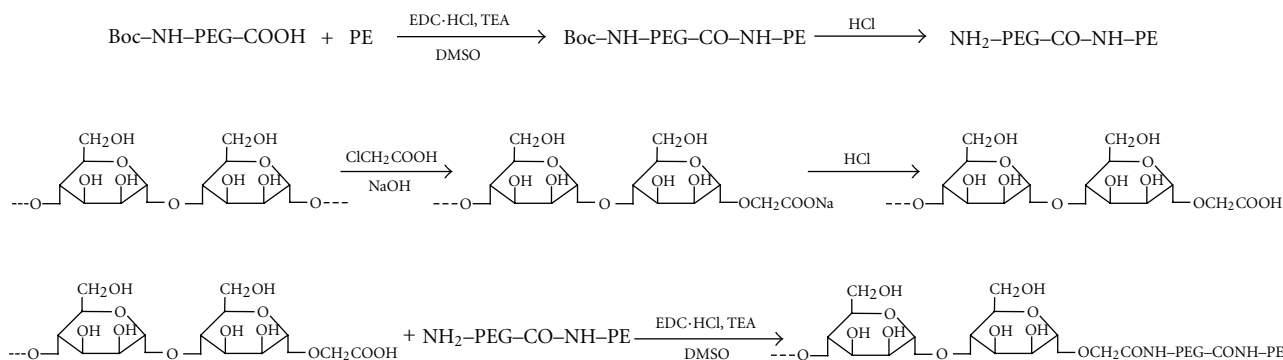
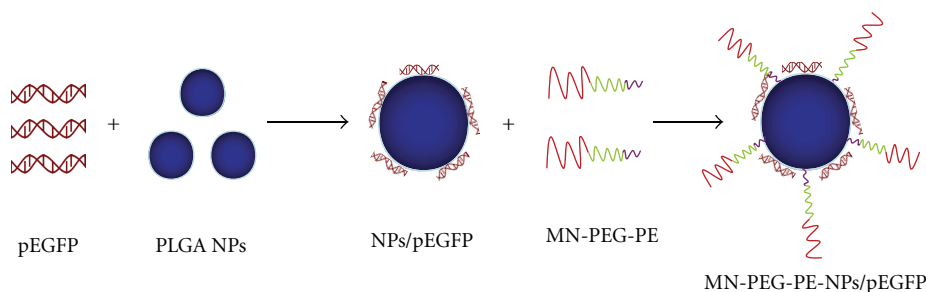FIGURE 1: General reaction scheme for the synthesis of MN-PEG-PE.

FIGURE 2: Preparation and modification of NPs-pEGFP complexes.

achieve. However, excessive modification could mask the surface change of the particle and cause the instability of the system. The complexes may disintegrate and pEGFP would detach from the vector and cause the notable decrease of the gene loading capacity, or the particles may aggregate and cause the mutation of particle size.

The particle sizes of the complexes at different ratios of MN-PEG-PE to NPs/pEGFP were detected to optimize the modification rate. The rates that obviously increase the particle sizes of the complexes are not suitable.

PicoGreen-fluorometry assay was used to further determine the appropriate modification rate of MN-PEG-PE ligands and also to quantitate the amount of pEGFP carried by the optimum modified NPs [30]. Different ratios of MN-PEG-PE to NPs/pEGFP were prepared and the pEGFP was isolated from the MN-PEG-PE- NPs/pEGFP by centrifugation at 1000 g, 4°C for 30 min. The concentration of pEGFP was determined by fluorescence, comparing with the supernatant from NPs. The amount of pEGFP loaded in the NPs was calculated according to the linear calibration curve of pEGFP.

2.6.2. Concanavalin A (Con A) Agglutination Study.

Binding of the terminal α-mannose residues to Con A causes agglutination of the complexes in solution, resulting in an increase in turbidity [31]. Con A agglutination assay was performed to indentify the MN-PEG-PE ligands successfully modified onto the NPs/pEGFP surface. 100 μL of MN-PEG-PE-NPs/pEGFP complexes was added into 500 μL of Con A (1 mg/mL) in PBS (pH 7.4) with 5 mM of calcium chloride (CaCl2) and 5 mM of magnesium chloride (MgCl2). The increase in turbidity at 360 nm (OD360) was monitored.

2.7. Isolation and Culture of KCs.

KCs were isolated from SD rats under pentobarbitone anaesthesia using the method described before [16]. Briefly, the rat's portal vein was cannulated and perfused with HBSS for 10 min, the liver was excised, and the perfusate was discarded. The liver was then perfused with 0.2% pronase, then with a recirculating solution of 0.05% pronase and 0.05% collagenase until the liver was digested. The liver was then cut into small pieces, suspended in the solution containing 0.02% pronase, 0.05% collagenase, and 0.005% DNase, and agitated. Following digestion, the liver homogenate was filtered through sterile gauze and centrifuged. The supernatant was removed and the pellet resuspended in Percoll gradient. Aliquots of this cell suspension were added to aliquots of Percoll gradient. These were carefully overlaid with HBSS and centrifuged. The nonparenchymal cell-enriched layer observed at the interface between the two layers was carefully harvested and diluted with HBSS. The suspension was then centrifuged to precipitate the KCs, which were then seeded into a 96-well microtiter plate in RPMI 1640 supplemented with 10% fetal bovine serum (FBS) and antibiotics. After incubation at 37°C for 2 h under 5% CO_2 atmosphere, the culture medium was replaced by 200 μL fresh RPMI 1640 to yield the purified KCs.

The isolated KCs were defined on the basis of the presence of phagocytosis of latex beads and positive immunostaining with antibody to the epitope ED2. With the abovementioned method, about 8.28×10^7/rat liver KCs were

Properties	Sample		
	NPs	NPs/pEGFP	MN-PEG-PE -NPs/pEGFP
Mean particle size (nm)	118.2 ± 3.4	149.5 ± 6.7	214.3 ± 8.3
Polydispersity index (PDI)	0.12 ± 0.06	0.21 ± 0.07	0.17 ± 0.08
Zeta potential (mV)	-28.36 ± 2.47	-36.17 ± 1.53	-20.28 ± 1.32

obtained; purity was about 91.8% (to 9.01×10^7/rat liver NPC). The isolated and purified rat KCs retained their *in vivo* morphological, biological, and immunological characteristics.

2.8. In Vitro Cytotoxicity Evaluation. The *in vitro* cytotoxicity of MN-PEG-PE-NPs/pEGFP in KCs was evaluated by MTT assay [32]. The KCs were incubated with MN-PEG-PE-NPs/pEGFP, unmodified NPs/pEGFP, and Lipo/pEGFP at various concentrations (10, 20, 50, 100, and 200 μg/mL) for 48 h at 37°C and 5% CO_2. The cell viability was then assessed by MTT assay. 5 mg/mL of MTT in PBS was then added to each well, and the plate was incubated for an additional 4 h at 37°C under the aforementioned 5% CO_2 atmosphere. Then the MTT containing medium was removed, and the crystals formed by living cells were dissolved in 100 μL DMSO. The absorbance at 570 nm was determined by a microplate reader. Untreated cells were taken as a control with 100% viability, and cells without the addition of MTT were used as a blank to calibrate the spectrophotometer to zero absorbance. The relative cell viability (%) compared to control cells was calculated using (Abs$_{sample}$/Abs$_{control}$) $\times$ 100.

2.9. In Vitro Transfection Analysis. For transfection efficiency analysis, the KCs were seeded into 24-well plates at a density of 1×10^5 cells/well in 1 mL of RPMI-1640 with 10% FBS. After about 24 h, the media were replaced with 400 μL transfection media containing MN-PEG-PE-NPs/pEGFP. Naked DNA, unmodified NPs/pEGFP, and Lipo/pEGFP were used as controls. The original incubation medium was replaced with 1 mL of complete medium after incubation at 37°C for 4 h under a 5% CO2 atmosphere. The cells were incubated and studied until 72 h after transfection. The fluorescent cells were observed using an inversion fluorescence microscope, at which time pictures were taken for the record.

2.10. In Vivo Gene Delivery. Adult male SD rats were divided into four groups (six rats in each group) and injected intravenously with 1 mL of MN-PEG-PE-NPs/pEGFP, NPs/pEGFP, Lipo/pEGFP, and naked pEGFP. At predetermined time intervals, the rats' KCs were isolated as described in Section 2.7. The cells were washed with 1 mL of PBS (100 g, 4°C for 5 min) and were detached with trypsin/EDTA. The supernatant was discarded and resuspended with 300 μL of PBS and added into the flow cytometry to determine the amount of KCs which has been successfully transfected.

2.11. Statistical Analysis. All studies were repeated three times, and all measurements were carried out in triplicate. Results were reported as means $\pm$ SD (SD = standard deviation). Statistical significance was analyzed using the Student's *t*-test. Differences between experimental groups were considered significant when the *P* value was less than 0.05 ($P < 0.05$).

3. Results

3.1. Characterization of pEGFP Loaded NPs. Mean particle size, polydispersity index (PDI), and zeta potential of NPs, NPs/pEGFP, and MN-PEG-PE-NPs/pEGFP were characterized and summarized in Table 1.

3.2. Optimization of the MN-PEG-PE Modification Rate. The particle sizes of the complexes at different ratios of MN-PEG-PE to NPs/pEGFP were detected and illustrated in Figure 3. With the increasing of the modification rate (from 5% to 20%), the particle size of NPs showed no obvious change (all around 210 mn). When the ratio of the ligands was increased to 35%, the particle size decreased to about 180mn, and then the size rose to 530 mn when the rate reached 45%.

PicoGreen-fluorometry assay was used to further determine the best modification rate of MN-PEG-PE ligands to the NPs/pEGFP carriers. Different ratios of MN-PEG-PE to NPs/pEGFP were prepared through the same method, and the amount of pEGFP was quantitated. Gene loading quantity(%)=(total amount of pEGFP − the amount of free pEGFP)/total amount of DNA $\times$ 100. The loading quantity of pEGFP loaded in the various modified NPs was calculated and displayed in Figure 4. Nonmodified NPs (0%) reach the gene loading quantity of 88.46%. With the increasing of the modification rate (from 5% to 20%), the loading amount of pEGFP showed no obvious change (all around 88%). When the ratio of the ligands was above 20%, the loading capacity was decreased, and observed only 36% gene carried at the ratio of 35%. Then the loading amount increased when the rate increased above 35%.

As the results proved clearly, the optimized rate of the MN-PEG-PE to NPs/pEGFP was 20%. This ratio was determined and used for the further experiments.

3.3. Determination of MN-PEG-PE Modification. Con A agglutination study was applied to further indentify the MN-PEG-PE ligands successfully modified onto the NPs/pEGFP surface. As stated above, the ratio of the MN-PEG-PE to NPs/pEGFP was 20% in this experiment and the following
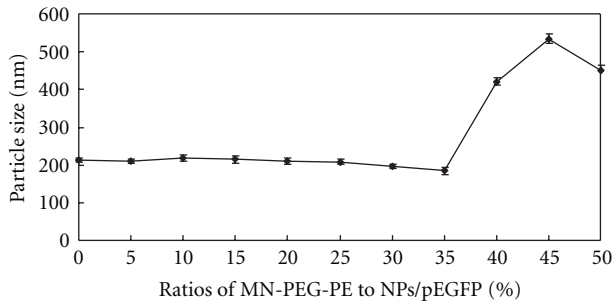
FIGURE 3: Optimization of MN-PEG-PE modification rate: Particle sizes determination.
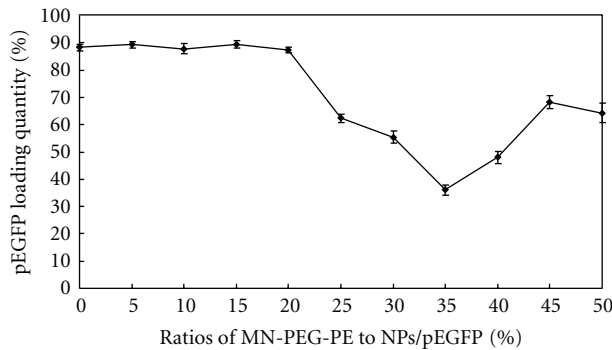

FIGURE 4: Optimization of MN-PEG-PE modification rate: Pico-Green-fluorometry assay.

▲ NPs
■ NPs/pEGFP
◆ MN-PEG-PE-NPs/pEGFP

FIGURE 5: The turbidity of NPs, NPs/pEGFP, and MN-PEG-PE-NPs/pEGFP at different time intervals.

☐ Lipofectamine2000/pEGFP
☐ NPs/pEGFP
■ MN-PEG-PE-NPs/pEGFP
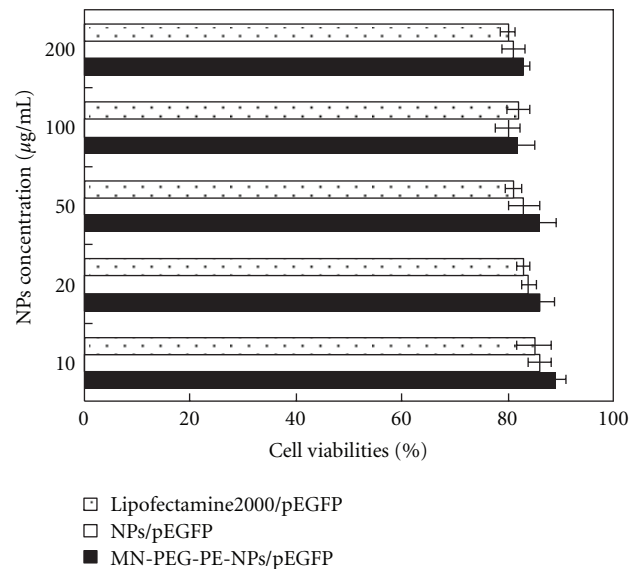
FIGURE 6: Cell viabilities of MN-PEG-PE-NPs/pEGFP and NPs/pEGFP.

investigation. The appearance in turbidity was monitored for 180 seconds (Figure 5).

MN-PEG-PE-NPs/pEGFP showed apparently increase in turbidity and reached 0.19 at the end of 180 s. NPs and NPs/pEGFP formulations appeared to show no significant increase in turbidity.

3.4. In Vitro Cytotoxicity Evaluation. *In vitro* cytotoxicity of MN-PEG-PE-NPs/pEGFP and non-modified NPs/pEGFP at various concentrations was evaluated by MTT assay. The cell viabilities of the NPs over the studied concentration range ($10\sim200\,\mu$g/mL) were between 80% and 100% compared with controls (Figure 6). MN-PEG-PE-NPs/pEGFP exhibited no higher cytotoxicity than NPs/pEGFP and Lipo/pEGFP at all concentrations ($P > 0.05$).

3.5. In Vitro Transfection Analysis. The *in vitro* transfection efficiencies of MN-PEG-PE-NPs/pEGFP and NPs/pEGFP in KCs after 72 h of transfection were analyzed. Naked DNA was used as a negative control. When compared with naked DNA and NPs/pEGFP, MN-PEG-PE-NPs/pEGFP had higher transfection efficiency at different time intervals (Figure 7).

3.6. In Vivo Gene Delivery. After intravenous injection with 1 mL of MN-PEG-PE-NPs/pEGFP, NPs/pEGFP, and naked pEGFP, the rats were euthanized and the KCs were isolated at 48 h and 72 h. Flow cytometry was applied to quantitate the amount of cells which have been successfully transfected.
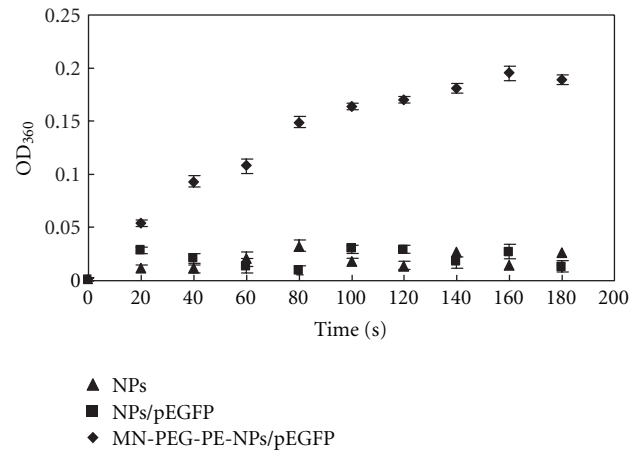
As shown in Figure 8, MN-PEG-PE-NPs/pEGFP displayed a remarkably higher transfection efficiency than non-modified NPs/pEGFP ($P < 0.05$) and naked pEGFP ($P < 0.05$), especially at 72 h after transfection.

4. Discussion

Biodegradable polymeric nanoparticles have been used frequently as gene delivery vehicles because they can be tailor made and surface modified to achieve both controlled drug release and active targeting. In the present study, novel conjugated mannan containing ligand MN-PEG-PE was synthesized and MN-PEG-PE modified bioadhesive PLGA nanoparticles were investigated as active targeting gene delivery system.

(a)

(b)

24   48   72
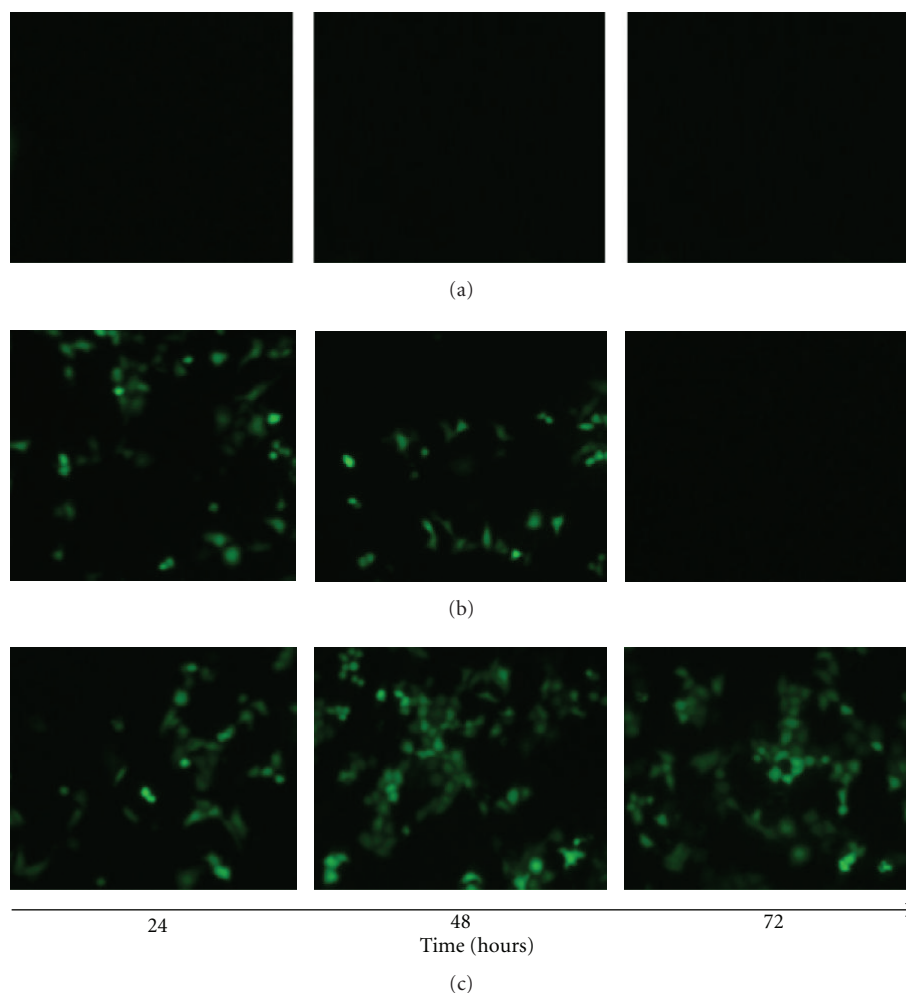Time (hours)

(c)

Figure 7: Fluorescent images of the KCs transfected with naked pEGFP (a), NPs/pEGFP (b), and MN-PEG-PE-NPs/pEGFP (c) at 24, 48, and 72 hours after transfection.

We began our investigation by synthesizing mannan containing PEG-PE ligand. Here, mannan is the target moiety which could bind to the mannose receptor (MR) in the macrophage, and PEG-PE is the spacer linked into the surface of NPs. It is reviewed that the length and flexibility of the spacer between the carbohydrate head group and nanocarrier surface mainly influence the target specificity and uptake of vectors by macrophages [33]. PEG-PE conjugates were reported, and TATp-PEG_{2000}-PE conjugates have been applied for the modification of nanocarriers to form active-targeting vectors [22], thus PEG_{2000}-PE was used at the anchor.

After the preparation of bioadhesive NPs and binding of NPs with pEGFP, MN-PEG-PE ligands were modified onto the NPs/pEGFP complexes by solvent diffusion method. The mannose group density is an important factor on the targeting efficiency [34] and vectors modified with higher content of sugar residues usually exhibit more efficient cellular recognition and internalization compare with lower sugar density. So theoretically, the more MN-PEG-PE ligands modified onto the carriers, the better targeted delivery ability

they will achieve. However, excessive modification could mask the surface change of the particle and cause the instability of the system. The complexes may disintegrate, and pEGFP would detach from the vector and cause the notable decrease of the gene loading capacity, or the particles may aggregate and cause the mutation of particle size. Particle size measurement was applied, and particle sizes of the complexes at different ratios of MN-PEG-PE to NPs/pEGFP were detected (Figure 3). With the increasing of the modification rate (from 5% to 20%), the particle size of NPs showed no obvious change (all around 210 mn). When the ratio increased to 35%, the size decreased to about 180mn, which may be explained by the separation of pEGFP form the vectors. When the rates continue to rise, the size rose to above 500 nm. This could be the proof of the aggregation of the NPs. PicoGreen-fluorometry assay was used to further determine the appropriate modification rate of MN-PEG-PE ligands and also to quantitate the amount of pEGFP carried by the optimum modified NPs. With the increasing of the modification rate (from 5% to 20%), the loading amount of pEGFP showed no obvious change (all around 88%). When
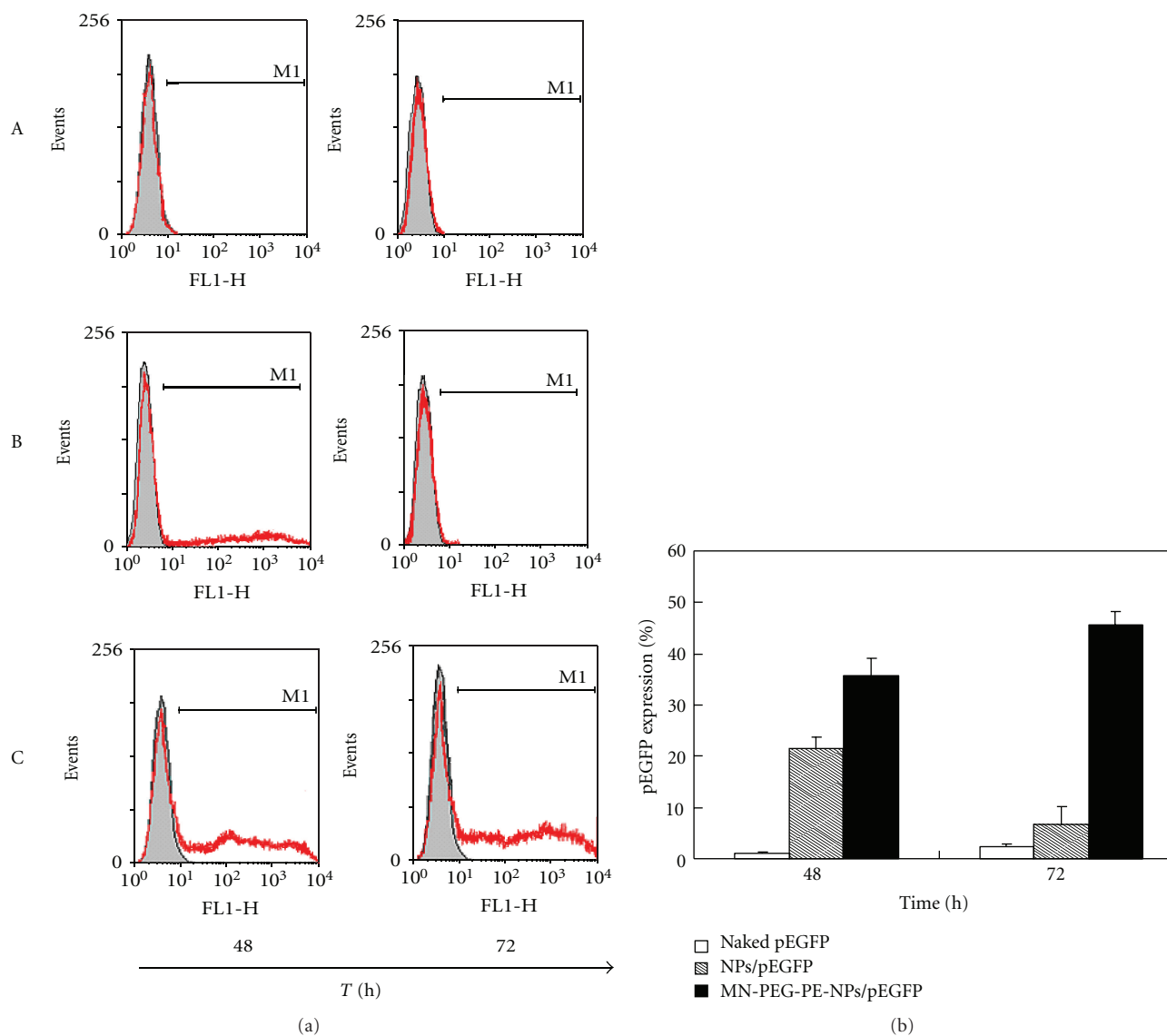
(a)

(b)

FIGURE 8: Flow cytometry analysis of KCs transfected by naked pEGFP (A), NPs/pEGFP (B) and MN-PEG-PE-NPs/pEGFP (C) *in vivo*.

the ratio of the ligands was above 20%, the loading capacity was decreased, and observed only 36% gene carried at the ratio of 35%. Then the loading amount increased when the rate increased above 35%. This could be explained by the aggregation of NPs reload with some of the pEGFP released form the NPs and caused the increase of loading amount to around 60%.

Con A was the first legume lectin recognized as one of the mannose-specific lectins and believed to play a role in recognition of mannose containing vectors [31, 35]. It was extensively used for the evaluating of glycoconjugates [36, 37]. Binding of the terminal α-mannose residues to Con A causes agglutination of the complexes in solution, resulting in an increase in turbidity. As shown in Figure 5, MN-PEG-PE-NPs/pEGFP showed apparent increase in turbidity and NPs and NPs/pEGFP formulations appeared to show no significant increase in turbidity. These could be the evidence

of the success of mannan containing ligands modified onto the nanoparticle surface.

Targeting macrophages is one of the promising therapeutic ways to treat genetic metabolic diseases such as human immunodeficiency virus infection because macrophages play a major role in the immune response to foreign antigen [38]. KCs are liver-specific resident macrophages that play an integral part in the physiological homeostasis of the liver. They have significant roles in acute and chronic responses of the liver to bacterial and viral infections and toxic or carcinogenic attack as well as mediating hepatotoxicity [39]. In this study, rat KCs were isolated and used as model cells for *in vitro* cytotoxicity evaluation and transfection analysis. MN-PEG-PE-NPs/pEGFP exhibited no higher cytotoxicity than NPs/pEGFP and Lipo/pEGFP at all concentrations. When compared with naked DNA and NPs/pEGFP, MN-PEG-PE-NPs/pEGFP had higher transfection efficiency at

different time intervals. This may be explained by the active targeting mechanism mediated by sugar-lectin recognition. The MN-PEG-PE-NPs/pEGFP were more likely to bind to the KCs through the MR on the cells and delivered the DNA more easily into the cells to express EGFP. The cells exhibited better green fluorescence at 48 and 72 hours. So 48 h and 72 h were chosen as the time points for the *in vivo* gene delivery study.

The *in vivo* gene delivery and expression studies were applied in the animal models to test the gene delivery ability of the modified gene vectors. After intravenous injection, the rats were euthanized and the KCs were isolated at 48 h and analyzed with flow cytometer. MN-PEG-PE-NPs/pEGFP displayed higher transfection efficiency (36.07%) than non-modified NPs/pEGFP (21.73%) and naked pEGFP (0.82%) at 48 h and remarkably higher transfection efficiency (47.15%) than non-modified NPs/pEGFP (8.16%) and naked pEGFP (1.31%) at 72 h. These results could demonstrate, MN-PEG-PE modified NPs had the ability to target liver KCs, deliver more genes into the cells and display higher transfection efficiency. The higher transfection efficiency at 72 h after injection could also illustrate the controlled-release ability of the vehicles. These evidences could strongly support the active targeting ability of mannan containing PEG-PE modified bioadhesive PLGA nanoparticles, and the resulting vectors would be very useful in gene delivery both *in vitro* and *in vivo*.
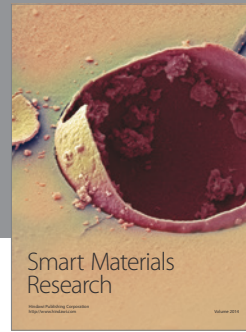
5. Conclusions

In the present study, we further confirmed the observations of other laboratories and the researches of our group that mannose-mediated targeting can successfully deliver genes into MR expressing cells. This investigation could also demonstrate that having mannose containing targeting ligands, such as MN-PEG-PE in this research, in DNA loaded PLGA NPs could significantly improve the transfection efficiency. By carefully formulating the carriers with an optimal ratio of MN-PEG-PE, efficient gene expressions were achieved in rats' KCs both *in vitro* and *in vivo*. These evidences could strongly support the active targeting ability of mannan containing PEG-PE modified bioadhesive PLGA nanoparticles, and the resulting vectors would be very useful in gene delivery both *in vitro* and *in vivo*.

References

[1] H. Boulaiz, J. A. Marchal, J. Prados, C. Melguizo, and A. Aránega, "Non-viral and viral vectors for gene therapy," *Cellular and Molecular Biology*, vol. 51, no. 1, pp. 3–22, 2005.

[2] X. B. Zhao and R. J. Lee, "Tumor-selective targeted delivery of genes and antisense oligodeoxyribonucleotides via the folate receptor," *Advanced Drug Delivery Reviews*, vol. 56, no. 8, pp. 1193–1204, 2004.

[3] H. Atkinson and R. Chalmers, "Delivering the goods: viral and non-viral gene therapy systems and the inherent limits on cargo DNA and internal sequences," *Genetica*, vol. 138, no. 5, pp. 485–498, 2010.

[4] V. P. Torchilin, "Multifunctional nanocarriers," *Advanced Drug Delivery Reviews*, vol. 58, no. 14, pp. 1532–1555, 2006.

[5] S. D. Li and L. Huang, "Surface-modified LPD nanoparticles for tumor targeting," *Annals of the New York Academy of Sciences*, vol. 1082, pp. 1–8, 2006.

[6] A. Kumari, S. K. Yadav, and S. C. Yadav, "Biodegradable polymeric nanoparticles based drug delivery systems," *Colloids and Surfaces B*, vol. 75, no. 1, pp. 1–18, 2010.

[7] K. Chaturvedi, K. Ganguly, A. R. Kulkarni et al., "Cyclodextrin-based siRNA delivery nanocarriers: a state-of-the-art review," *Expert Opinion on Drug Delivery*, vol. 8, no. 11, pp. 1455–1468, 2011.

[8] W. E. Rudzinski and T. M. Aminabhavi, "Chitosan as a carrier for targeted delivery of small interfering RNA," *International Journal of Pharmaceutics*, vol. 399, no. 1-2, pp. 1–11, 2010.

[9] D. B. Shenoy and M. M. Amiji, "Poly(ethylene oxide)-modified poly(ε-caprolactone) nanoparticles for targeted delivery of tamoxifen in breast cancer," *International Journal of Pharmaceutics*, vol. 293, no. 1-2, pp. 261–270, 2005.

[10] R. C. Mundargi, V. R. Babu, V. Rangaswamy, P. Patel, and T. M. Aminabhavi, "Nano/micro technologies for delivering macromolecular therapeutics using poly(d,l-lactide-co-glycolide) and its derivatives," *Journal of Controlled Release*, vol. 125, no. 3, pp. 193–209, 2008.

[11] S. A. Agnihotri, N. N. Mallikarjuna, and T. M. Aminabhavi, "Recent advances on chitosan-based micro- and nanoparticles in drug delivery," *Journal of Controlled Release*, vol. 100, no. 1, pp. 5–28, 2004.

[12] S. M. Moghimi, A. C. Hunter, and J. C. Murray, "Long-circulating and target-specific nanoparticles: theory to practice," *Pharmacological Reviews*, vol. 53, no. 2, pp. 283–318, 2001.

[13] K. S. Soppimath, T. M. Aminabhavi, A. R. Kulkarni, and W. E. Rudzinski, "Biodegradable polymeric nanoparticles as drug delivery devices," *Journal of Controlled Release*, vol. 70, no. 1-2, pp. 1–20, 2001.

[14] J. Panyam and V. Labhasetwar, "Biodegradable nanoparticles for drug and gene delivery to cells and tissue," *Advanced Drug Delivery Reviews*, vol. 55, no. 3, pp. 329–347, 2003.

[15] W. Zou, C. Liu, Z. Chen, and N. Zhang, "Studies on bioadhesive PLGA nanoparticles: a promising gene delivery system for efficient gene therapy to lung cancer," *International Journal of Pharmaceutics*, vol. 370, no. 1-2, pp. 187–195, 2009.

[16] F. Zhou, F. Kong, L. Ge, X. Liu, and N. Huang, "Mannan-modified PLGA nanoparticles for targeted gene delivery," *International Journal of Photoenergy*, vol. 2012, Article ID 926754, 7 pages, 2012.

[17] L. E. Van Vlerken, T. K. Vyas, and M. M. Amiji, "Poly(ethylene glycol)-modified nanocarriers for tumor-targeted and intracellular delivery," *Pharmaceutical Research*, vol. 24, no. 8, pp. 1405–1414, 2007.

[18] V. P. Torchilin, "Micellar nanocarriers: pharmaceutical perspectives," *Pharmaceutical Research*, vol. 24, no. 1, pp. 1–16, 2007.

[19] A. N. Lukyanov, Z. Gao, L. Mazzola, and V. P. Torchilin, "Polyethylene glycol-diacyllipid micelles demonstrate increased accumulation in subcutaneous tumors in mice," *Pharmaceutical Research*, vol. 19, no. 10, pp. 1424–1429, 2002.

[20] V. P. Torchilin, "Recent advances with liposomes as pharmaceutical carriers," *Nature Reviews Drug Discovery*, vol. 4, no. 2, pp. 145–160, 2005.

[21] L. Yang, L. Wang, X. Q. Su et al., "Suppression of ovarian cancer growth via systemic administration with liposome-encapsulated adenovirus-encoding endostatin," *Cancer Gene Therapy*, vol. 17, no. 1, pp. 49–57, 2010.

[22] R. M. Sawant, J. P. Hurley, S. Salmaso et al., "'SMART' drug delivery systems: double-targeted pH-responsive pharmaceutical nanocarriers," *Bioconjugate Chemistry*, vol. 17, no. 4, pp. 943–949, 2006.

[23] J. A. Reddy, C. Abburi, H. Hofland et al., "Folate-targeted, cationic liposome-mediated gene transfer into disseminated peritoneal tumors," *Gene Therapy*, vol. 9, no. 22, pp. 1542–1560, 2002.

[24] O. Penate Medina, M. Haikola, M. Tahtinen et al., "Liposomal tumor targeting in drug delivery utilizing MMP-2- and MMP-9-binding ligands," *Journal of Drug Delivery*, vol. 2011, Article ID 160515, 9 pages, 2011.

[25] L. Yang, L. Cheng, Y. Wei, and L. Tian, "Synthesis of N-[2-(cholesteryloxycarbonylamino) ethyl] carbamoylmethylated mannan," *Journal of Sichuan University*, vol. 34, no. 4, pp. 730–732, 2003.

[26] S. J. Ahn, J. Costa, and J. R. Emanuel, "PicoGreen quantitation of DNA: effective evaluation of samples pre- or post-PCR," *Nucleic Acids Research*, vol. 24, no. 13, pp. 2623–2625, 1996.

[27] J. Ye, A. Wang, C. Liu, Z. Chen, and N. Zhang, "Anionic solid lipid nanoparticles supported on protamine/DNA complexes," *Nanotechnology*, vol. 19, no. 28, Article ID 285708, 2008.

[28] W. Wijagkanalan, S. Kawakami, M. Takenaga, R. Igarashi, F. Yamashita, and M. Hashida, "Efficient targeting to alveolar macrophages by intratracheal administration of mannosylated liposomes in rats," *Journal of Controlled Release*, vol. 125, no. 2, pp. 121–130, 2008.

[29] W. Yu, C. Liu, Y. Liu, N. Zhang, and W. Xu, "Mannan-modified solid lipid nanoparticles for targeted gene delivery to alveolar macrophages," *Pharmaceutical Research*, vol. 27, no. 8, pp. 1584–1596, 2010.

[30] N. Adjimatera, T. Kral, M. Hof, and I. S. Blagbrough, "Lipopolyamine-mediated single nanoparticle formation of calf thymus DNA analyzed by fluorescence correlation spectroscopy," *Pharmaceutical Research*, vol. 23, no. 7, pp. 1564–1573, 2006.

[31] A. Barre, Y. Bourne, E. J. M. Van Damme, W. J. Peumans, and P. Rougé, "Mannose-binding plant lectins: different structural scaffolds for a common sugar-recognition process," *Biochimie*, vol. 83, no. 7, pp. 645–651, 2001.

[32] Y. Gao, W. Gu, L. Chen, Z. Xu, and Y. Li, "A multifunctional nano device as non-viral vector for gene delivery: in vitro characteristics and transfection," *Journal of Controlled Release*, vol. 118, no. 3, pp. 381–388, 2007.

[33] W. Yu, N. Zhang, and C. Li, "Saccharide modified pharmaceutical nanocarriers for targeted drug and gene delivery," *Current Pharmaceutical Design*, vol. 15, no. 32, pp. 3826–3836, 2009.

[34] W. Yeeprae, S. Kawakami, F. Yamashita, and M. Hashida, "Effect of mannose density on mannose receptor-mediated cellular uptake of mannosylated O/W emulsions by macrophages," *Journal of Controlled Release*, vol. 114, no. 2, pp. 193–201, 2006.

[35] J. B. Summer and S. F. Howell, "The identification of the hemagglutinin of the jack bean with concanavalin A," *Journal of Bacteriology*, vol. 32, pp. 227–237, 1936.

[36] J. N. Kizhakkedathu, A. L. Creagh, R. A. Shenoi et al., "High molecular weight polyglycerol-based multivalent mannose conjugates," *Biomacromolecules*, vol. 11, no. 10, pp. 2567–2575, 2010.

[37] M. L. Wolfenden and M. J. Cloninger, "Mannose/glucose-functionalized dendrimers to investigate the predictable tunability of multivalent interactions," *Journal of the American Chemical Society*, vol. 127, no. 35, pp. 12168–12169, 2005.

[38] M. Yamada, M. Nishikawa, S. Kawakami et al., "Tissue and intrahepatic distribution and subcellular localization of a mannosylated lipoplex after intravenous administration in mice," *Journal of Controlled Release*, vol. 98, no. 1, pp. 157–167, 2004.

[39] H. Kitani, T. Takenouchi, M. Sato, M. Yoshioka, and N. Yamanaka, "A novel isolation method for macrophage-like cells from mixed primary cultures of adult rat liver cells," *Journal of Immunological Methods*, vol. 360, no. 1-2, pp. 47–55, 2010.

Journal of
Nanotechnology

International Journal of
Corrosion

International Journal of
Polymer Science

Smart Materials
Research

Journal of
Composites

BioMed
Research International

Journal of
Metallurgy

Journal of
Materials

Hindawi

Submit your manuscripts at
http://www.hindawi.com

Journal of
Nanoparticles

Advances in
Materials Science and Engineering

Scientifica

Journal of
Nanomaterials

The Scientific
World Journal

International Journal of
Biomaterials

Journal of
Nanoscience

Journal of
Coatings

Journal of
Crystallography

Journal of
Ceramics

Journal of
Textiles